Published in final edited form as:

J Neurochem. 2021 March ; 156(5): 658–673. doi:10.1111/jnc.15260.

Pimavanserin, a $5HT_{2A}$ receptor inverse agonist, rapidly suppresses Aβ production and related pathology in a mouse model of Alzheimer's disease

Carla M. Yuede[1,2,3], **Clare E. Wallace**[1,2,3], **Todd A. Davis**[1,2,3], **Woodrow D. Gardiner**[1,2,3], **Jane C. Hettinger**[1,2,3], **Hannah M. Edwards**[1,2,3], **Rachel D. Hendrix**[1,2,3], **Brookelyn M. Doherty**[1,2,3], **Kayla M. Yuede**[1,2,3], **Ethan S. Burstein**[4], **John R. Cirrito**[1,2,3]

[1]Department of Neurology, Washington University School of Medicine, St. Louis, MO, USA

[2]Knight Alzheimer's Disease Research Center, Washington University School of Medicine, St. Louis, MO, USA

[3]Hope Center for Neurological Disorders, Washington University School of Medicine, St. Louis, MO, USA

[4]ACADIA Pharmaceuticals Inc, San Diego, CA, USA

Abstract

Amyloid-β (Aβ) peptide aggregation into soluble oligomers and insoluble plaques is a precipitating event in the pathogenesis of Alzheimer's disease (AD). Given that synaptic activity can regulate Aβ generation, we postulated that $5HT_{2A}$-Rs may regulate Aβ as well. We treated APP/PS1 transgenic mice with the selective $5HT_{2A}$ inverse agonists M100907 or Pimavanserin systemically and measured brain interstitial fluid (ISF) Aβ levels in real-time using in vivo microdialysis. Both compounds reduced ISF Aβ levels by almost 50% within hours, but had no effect on Aβ levels in $5HT_{2A}$-R knock-out mice. The Aβ-lowering effects of Pimavanserin were blocked by extracellular-regulated kinase (ERK) and NMDA receptor inhibitors. Chronic administration of Pimavanserin by subcutaneous osmotic pump to aged APP/PS1 mice significantly reduced CSF Aβ levels and Aβ pathology and improved cognitive function in these mice. Pimavanserin is FDA-approved to treat Parkinson's disease psychosis, and also has been shown to reduce psychosis in a variety of other dementia subtypes including Alzheimer's disease. These data demonstrate that Pimavanserin may have disease-modifying benefits in addition to its efficacy against neuropsychiatric symptoms of Alzheimer's disease.

Correspondence: John R. Cirrito, Department of Neurology, Washington University, Campus Box 8111, 660 South Euclid Avenue, St. Louis, MO 63110, USA. cirritoj@wustl.edu, Ethan S. Burstein, ACADIA Pharmaceuticals Inc., 12830 El Camino Real, Suite 400, San Diego, CA, 92130, USA. eburstein@acadia-pharm.com.

CONFLICT OF INTEREST

This work was initiated in collaboration with, and was partially financially supported by, ACADIA Pharmaceuticals Inc. ESB is an employee of ACADIA Pharmaceuticals Inc.

SUPPORTING INFORMATION

Additional supporting information may be found online in the Supporting Information section.

Keywords

$5HT_{2A}$ receptors; Alzheimer's disease; amyloid-β; microdialysis; Pimavanserin; serotonin receptors

1 | INTRODUCTION

Among the numerous pathophysiological changes that occur in Alzheimer's disease (AD), this disorder is characterized by two major pathologies: amyloid-β (Aβ) plaques and tau neurofibrillary tangles. It appears that Aβ accumulation is the initiating factor that leads to AD, while tau tangles play a critical role in neuronal death and AD progression (Holtzman et al., 2011). Early in disease pathogenesis, soluble Aβ monomers aggregates into soluble Aβ oligomers and insoluble Aβ plaques, both of which cause synaptic dysfunction and kill neurons under certain conditions. Conversion of Aβ from its normal soluble form into these toxic conformations is concentration-dependent; higher concentrations of Aβ are much more prone to aggregate (Bero et al., 2011; Lomakin et al., 1997). Amyloid plaques and soluble Aβ oligomers exist within the brain extracellular space, or interstitial fluid (ISF). Soluble Aβ within the ISF is one source that contributes to these toxic species (Bero et al., 2011; Yan et al., 2009). Consequently, maintaining low Aβ levels, particularly within the ISF, should limit creation of toxic forms of Aβ.

Aβ levels are regulated by multiple mechanisms. Synaptic transmission generates Aβ which is then released into the ISF (Cirrito et al., 2005, 2008; Verges et al., 2011). Additionally, the activation of certain neurotransmitter receptors can alter APP processing which impacts Aβ generation (Cirrito et al., 2011; Hettinger et al., 2018; Verges et al., 2011). For instance, in mice and humans that NMDA and $G_{\alpha s}$-coupled serotonin receptors $5HT_4$, $5HT_6$ and $5HT_7$ activate the ERK signaling cascade which increases α-secretase enzymatic activity to reduce Aβ levels (Cirrito et al., 2011; Fisher et al., 2016; Hoey et al., 2009; Lesne et al., 2005; Nitsch et al., 1996; Sheline et al., 2014; Verges et al., 2011).

$5HT_{2A}$-Rs are G-protein-coupled receptors that are highly expressed predominantly in postsynaptic compartments throughout the central nervous system (CNS), with limited presynaptic localization (Beliveau et al., 2017; Jakab & Goldman-Rakic, 1998; Miner et al., 2003; Willins et al., 1997). They couple to $G_{\alpha q}$ subunits which regulate a multitude of signaling pathways including ERK, and influence signaling through other neurotransmitter receptors, such as AMPA and NMDA receptors (Farber et al., 1998; Zhang & Marek, 2008). 5-HT_{2A}-Rs are targets of psychedelic drugs (Preller et al., 2018), and nearly all atypical antipsychotic drugs (Weiner et al., 2001), which activate or suppress receptor activity, respectively. In addition, deletion of $5HT_{2A}$-Rs affects sleep architecture (Popa et al., 2005), and drugs that suppress $5HT_{2A}$-R activity promote slow-wave sleep (SWS) (Ancoli-Israel et al., 2011; Patel et al., 2018; Popa et al., 2005; Vanover & Davis, 2010). A reciprocal relationship between SWS and Aβ accumulation has been demonstrated, with interruptions in SWS leading to Aβ accumulation, and augmentation of SWS lowering Aβ accumulation (Ju et al., 2017, 2019). For these reasons, we sought to determine if suppressing $5HT_{2A}$-R activity with compounds that selectively target 5-HT_{2A}-Rs would also regulate Aβ levels.

Pimavanserin (Pim), is a selective $5HT_{2A}$-R inverse agonist and functional antagonist (Hacksell et al., 2014; Vanover et al., 2006) with lesser activity at $5HT_{2C}$-Rs, and no appreciable activity at over 70 other targets, that is FDA-approved to treat hallucinations and delusions associated with Parkinson's disease (Cummings et al., 2018). M100907 is known as a highly selective $5HT_{2A}$-R antagonist, lacking appreciable activity at any other targets including $5HT_{2C}$-Rs (Kehne et al., 1996; Weiner et al., 2001), and also behaves as a $5HT_{2A}$-R inverse agonist (Weiner et al., 2001). We treated APP/PS1 mice with either Pim or M100907. We find that both agents rapidly reduce brain ISF Aβ levels by 40%–50%, effects that are also very similar in wildtype (WT) mice, but completely abolished in $5HT_{2A}$-R knockout (KO) mice. Interestingly, the effect of Pim on Aβ is also completely blocked if NMDA-Rs are inhibited, suggesting that NMDA-Rs act downstream to mediate the effects of 5-HT2A-Rs on Aβ production. Chronic administration of Pim to aged APP/PS1 mice that already contain Aβ plaques significantly reduces further plaque accumulation and ameliorates behavioral deficits, suggesting that Pim may help treat the underlying disease as well as the neuropsychiatric symptoms of AD.

2 | MATERIALS AND METHODS

This study was not pre-registered.

2.1 | Animals

All experiment protocols using animals were performed ethically and in accordance to the guidelines established by the Institutional Animal Care and Use Committee at Washington University. We bred *APPswe/PS1ΔE9* hemizygous mice (Jackson Laboratory, RRID: MMRRC_034829.JAX) (Savonenko et al., 2003) to wild type C3H/B6 mice and aged the *APP/PS1*$^{\pm}$ offspring to 2–3.5 months for microdialysis experiments or to 10 months for pathology studies. Initially 265 mice were allocated for this study, with a total of 260 mice presented in figure data. For acute microdialysis studies, 3–8 mice (mixed sex) were used per group. For the chronic Pim administration study, initial group sizes were 16–20 (mixed sex), with final group sizes being 14–20. Mice were housed in static cages with 3–5 mice per cage and screened for APPswe and PS1ΔE9 transgenes by PCR from toe DNA. Male and female mice were used for all studies and littermates were randomized into treatment groups. For in vivo microdialysis, littermates were arbitrarily assigned to treatment groups for each set of 4 mice within an experimental run. For chronic treatment studies, simple randomization by dice roll was used to separate littermates by genotype and sex into treatment groups. $5HT_{2A}$-R knockout mice have been described previously (Halberstadt et al., 2009).

2.2 | Compounds

All pharmacological and chemical agents were purchased from Sigma-Aldrich unless otherwise noted. All compounds that were delivered to the hippocampus via reverse microdialysis were diluted in microdialysis perfusion buffer which consisted of artificial CSF with 0.15% bovine serum albumin (Sigma, Cat# 05470) filtered through a 0.22 μm membrane. M100907, FR180204, and KT5720 were purchased from Tocris Bioscience

(Cat#'s 4173; 3706; 1288; Ellisville). LY411575 was purchased from Sigma (Cat# SML0506). Pimavanserin was provided by ACADIA Pharmaceuticals Inc.

2.3 | In vivo Aβ microdialysis

In vivo microdialysis to measure brain ISF Aβ in the hippocampus of freely moving APP/PS1 mice was performed similar to previously described (Cirrito et al., 2003; Fisher et al., 2016; Hettinger et al., 2018). This method captures soluble molecules in the extracellular fluid that are below the 38 kDa molecular weight cutoff of the probes. Under volatile isoflurane anesthetic (1%–4%) applied through a stereotaxic nose cone, guide cannula (MBR-style Cat# MD-2255; Bioanalytical Systems) were cemented above the left hippocampus (3.1 mm behind bregma, 2.5 mm lateral to midline, and 1.2 mm below dura at a 12° angle). Isoflurane provides a stable and quick-onset/offset of anesthesia over the course of a 30 min surgery. Two millimeter microdialysis probes were inserted through the guides so their membranes were completely contained in the hippocampus (38 kDa BR-2; Cat# MD-2212, Bioanalytical Systems). Microdialysis buffer was aCSF (perfusion buffer in mM: 1.3 $CaCl_2$, 1.2 $MgSO_4$, 3 KCl, 0.4 KH_2PO_4, and 122 NaCl, pH 7.35) containing 0.15% BSA that was filtered through a 0.22 μM membrane. The flow rate was 1.0 μl/min. Samples were collected every 60 or 90 min into a refrigerated fraction collector (Univentor Limited) in polypropylene tubes and assessed for $Aβ_{x-40}$ or $Aβ_{x-42}$ by sandwich ELISA. Guide cannula surgeries generally occurred in the afternoon 24 hr before microdialysis was initiated. After the microdialysis probes were inserted into the brain, mice recovered for at least 6 hr then baseline Aβ levels were measured. Initial administration occurred in the morning, usually between 9–10 a.m. Basal ISF Aβ levels were defined as the mean concentration of Aβ over the 9 hr preceding drug administration. All Aβ values were normalized to the basal Aβ concentration for each animal. After establishing baseline ISF Aβ, pharmaceutical agents delivered by reverse microdialysis were diluted in microdialysis perfusion buffer and infused directly into the hippocampus. Mice were sacrificed by cardiac perfusion following 1%–4% volatile isoflurane anesthesia applied in a gas chamber. The primary endpoints of this study were Aβ plaque load and biochemical measures of brain Aβ content. Behavioral assays were secondary endpoints.

Pain and distress were minimized in these studies. Any mouse that seemed lethargic or stopped eating/drinking following microdialysis guide cannula surgery or during the experiment was sacrificed immediately. As approved in our IACUC protocol, neither non-steroidal anti-inflammatory drugs nor opioid analgesics were administered to the mice, as previous studies have shown each of these classes of agents alters APP processing into Aβ which would have altered the results of these studies (Cai & Ratka, 2012; Eriksen et al., 2003).

2.4 | Aβ elimination half-life

ISF Aβ half-life was determined as described (Cirrito et al., 2003) and microdialysis probes were inserted as described above. New steady-state ISF Aβ levels were established following treatment with Pimavanserin (1 mg/kg) or vehicle (PBS) by reverse microdialysis for nine hours. At the end of 9 hr, mice were co-administered a potent, blood-brain permeable γ-secretase inhibitor, LY411575, (Grimwood et al., 2005), (3 mg/kg diluted in

50:50 PBS:PEG400) intraperitoneally to rapidly block Aβ production. Microdialysis samples were collected every 60 min for 6 hr then assayed for $Aβ_{x-40}$ by ELISA. The half-life of ISF Aβ was calculated based on the slope of the semi-log plot of % change in Aβ versus time (Cirrito et al., 2003). Only Aβ values that were continually decreasing were included in half-life analysis (the first 3 hr following LY411575 administration).

2.5 | Aβ sandwich ELISA

ISF $Aβ_{x-40}$ and $Aβ_{x-42}$ levels were measured using sandwich ELISAs as described (Hettinger et al., 2018). This ELISA detects both human and murine Aβ. A mouse anti-$Aβ_{40}$ antibody (mHJ2; 10 μg/ml) or mouse anti-$Aβ_{42}$ antibody (mHJ7.4; 10 μg/ml) against the C-terminus of Aβ was used to capture peptides and a biotinylated central domain antibody (mHJ5.1; 75 ng/ml) was used to detect them. This was followed by a streptavidin poly-HRP-40 assay to measure Aβ concentration (Cat# 65R-S104PHRP, Fitzgerald Industries). All steps included washes with PBS containing 0.05% Tween-20. The standard curve for the ELISA was recombinant $Aβ_{40}$ or $Aβ_{42}$ (Cat# AS-24236; AS-20276, Anaspec) taken from a stock in formic acid to remove pre-formed aggregates. ELISA sample buffers included sufficient Tris to neutralize pH of the formic acid. ELISAs were developed using Super Slow ELISA TMB (Cat# T5569, Sigma-Aldrich) and absorbance read on a Bio-Tek Epoch plate reader at 650 nm.

2.6 | Chronic Pimavanserin administration

Beginning at 6 months of age, APP/PS1 hemizygous male and female mice were implanted with Alzet osmotic pumps (model 2006) into the subcutaneous space on the animal back. Littermates were arbitrarily assigned into three treatment groups. One group was sacrificed at 6 months of age as a measure of plaques at the “Start” of the study. For the other two groups, pumps were loaded with vehicle or Pimavanserin (PBS or 3mg kg day^{-1} in PBS, respectively). Pumps were replaced every 2.5–5 weeks; alternating location of the pump on either side of the back. Mice were housed 3–5 animals per cage. Twice mice assigned to the vehicle-group and three assigned to the Pim-group died from fighting or during osmotic pump implantation; not because of drug treatment. The original groups were intentionally overpowered to account for attrition over time, so no mice were replaced in the study. No adverse events were noted in either group during the course of the study. Body weights for each group were not significantly different (mean ± *SD*: APP PIM 40.77 ± 6.296; APP VEH 40.42 ± 7.71; WT PIM 37.73 ± 6.098; WT VEH 39.15 ± 7.931). At 10 months of age, mice were sacrificed with CSF drawn from the cisterna magna (DeMattos et al., 2002) followed by transcardial perfusion of chilled PBS with 0.3% heparin. One hemisphere of the brain was post-fixed overnight in 4% paraformaldehyde followed by processing for histological analysis of Aβ plaque burden. The other hemisphere had the hippocampus and cortex micro-dissected for biochemical analysis of brain Aβ levels.

Pain and distress were minimized in these studies. Mice that had severe infections surrounding the osmotic pump were sacrificed immediately. As approved in our IACUC protocol, neither non-steroidal anti-inflammatory drugs nor opioid analgesics were administered to the mice, as previous studies have shown each of these classes of agents

alters APP processing into Aβ which would have altered the results of these studies (Cai & Ratka, 2012; Eriksen et al., 2003).

2.7 | Tissue extraction of Aβ

To evaluate various pools of brain Aβ we performed a sequential extraction of tissue with PBS, 1% Triton X-100 in PBS, then 5 M guanidine to grossly assess the extracellular-enriched fraction, the membrane-bound and intracellular fraction, and the insoluble fraction, respectively. All lysis buffers were chilled to 4°C and contained protease inhibitors without EDTA. Tissue was lysed at a 1:10 wet weight/volume ratio. PBS and Triton X-100 extractions were performed by mechanical dounce homogenization while the guanidine extraction was performed with sonication to maximally solubilize remaining Aβ within the tissue. Tissue was spun in a microcentrifuge at 21,000 g for 15 min at 4°C following each extraction.

2.8 | Quantitative analyses of Aβ deposition

Brain hemispheres were placed in 30% sucrose before freezing and cutting on a freezing sliding microtome. Serial coronal sections of the brain at 50 mm intervals were collected from the rostral anterior commisure to caudal hippocampus as landmarks. Sections were stained with biotinylated anti-Aβ antibody, mHJ3.4 (hybridomas were a kind gift from Dr David Holtzman, Washington University). Stained brain sections were scanned with a NanoZoomer slide scanner (Hamamatsu Photonics). For quantitative analyses of mHJ3.4-biotin staining, scanned images were exported with NDP viewer software (Hamamatsu Photonics) and converted to 8 bit grayscale using ACDSee Pro 3 software (ACD Systems). Converted images were thresholded to highlight plaques and then analyzed by “Analyze Particles’ function in the ImageJ software (National Institutes of Health, RRID:SCR_003070) (Kim et al., 2007). Identified objects after thresholding were individually inspected to confirm the object as a plaque or not. Three brain sections per mouse, each separated by 300 mm, were used for quantification. These sections correspond roughly to sections at Bregma −1.7, −2.0, and −2.3 mm in the mouse brain atlas. The average of three sections was used to represent a plaque load for each mouse. For analysis of Aβ plaque in the cortex, the cortex immediately dorsal to the hippocampus was assessed. All analyses were performed in a blinded manner by two independent researchers; their values for each mouse were averaged then plotted for statistical analyses. The data that was statistically analyzed and plotted represents the average plaque load per section between the two researchers.

2.9 | SDS-PAGE/western blot

Hippocampus from APP/PS1 mice treated with Pimavanserin for 12 hr was lysed in 1% Triton X-100, 0.1% SDS in PBS by sonication. Twenty microgram of total protein was loaded per lane on SDS-PAGE gels. SDS-PAGE was performed using 16% Novex Tricine gels (Cat# EC66955, Invitrogen) under reducing conditions. Samples were loaded onto the gels in alternating basal and drug-treated samples. Nitrocellulose blots were blocked in 3% bovine serum albumin and probed with either rabbit-anti-APP antibody directed against the C-terminus (Cat# SAB3500274, Sigma-Aldrich) or mouse-anti-GAPDH (Cat# G8795, Sigma-Aldrich) followed by a mouse-anti-rabbit HRP (Cat# 211-032-171, Jackson

ImmunoResearch) or a sheep-anti-mouse antibody (Cat# 45-000-692, GE Life Sciences) in 1% bovine serum albumin. Blots were washed in 0.05% Tween-20 in PBS three times for at least 5 min each. Bands were detected with Lumigen-TMA6 (Cat# TMA, Amersham) and captured digitally using the Kodak ImageStation 440CF. Densitometry was performed using the Kodak 1D Image Analysis software. Tissue protein levels were normalized to GAPDH for each lane, then normalized to % vehicle for each blot, followed by data from two blots being combined for analysis.

2.10 | Secretase enzymatic activity assays

Enzymatic activity of α-secretase and β-secretase was measured using FRET-based cleavage assays (Cat# FP001, FP002, R&D Systems). For studies in young mice (3–4 months old), hippocampal tissue was isolated from APP/PS1 hemizygous mice treated with Pimavanserin (1mg/kg) or vehicle (PBS) and sacrificed 12 hr later. Tissue was lysed in 1% Triton-X 100 with sonication. Cell extracts were incubated with secretase-specific peptides conjugated to the reporter molecules EDANS and DABCYL for 15–30 min. EDANS fluorescence was read on a Synergy 2 microtiter plate reader (BioTek, Winooski, VT).

2.11 | Behavior tests

The behavioral performance of APP/PS1 ± mice and WT littermates was evaluated at 12 months of age, following 4 months of treatment (n = 15 per group). Sample sizes were based off of previous experience with variability in behavior tests and estimated to detect ~ 15% difference between groups. The open field test was used to measure differences in general activity or emotionality between the genotypes and treatments. A battery of sensorimotor tests was used to screen for differences in balance, coordination, motor function, or other non-associative factors that could confound interpretation of the cognitive tests. Spatial learning and memory were evaluated in the Morris Water Maze task, and recognition memory was assessed in a novel object recognition task based on previously published methods (Wozniak et al., 2004, 2013; Yuede et al., 2009).

2.12 | General design of behavioral tests

All behavioral testing was conducted during the light cycle, by a female experimenter blinded to experimental group. Run order IDs were assigned by an experimenter different from the experimenter conducting the testing and cage cards did not contain genotype or treatment information. All equipment was cleaned with 2% chlorhexidine diacetate or 70% ethanol between animals. Room temperature and humidity was kept within a consistent range during testing (68–74F°, 30%–50%). The order of tests conducted were as follows: open field, sensorimotor battery, elevated plus maze, water maze, and novel object recognition.

2.12.1 | Open field activity/exploratory behavior—General activity levels and exploratory behavior was quantified over a 60-min period in an open-field (41 × 41×38.5 cm high) constructed of Plexiglas and surrounded by computerized photobeam instrumentation (Kinder Scientific, LLC). General activity variables (total ambulations, rearings, time at rest) along with measures of emotionality, including time spent, distance traveled, and entries made into the central zone were analyzed.

2.12.2 | Sensorimotor battery—Walking initiation, ledge, platform, pole, and inclined and inverted screen tests were performed as described previously (Wozniak et al., 2004). Time in each task was manually recorded. The average for two trials was used for analyses. Test duration was 60s, except for the pole test, which was extended to 120s. For walking initiation, time for an animal to leave a 21 × 21 cm square on a flat surface was recorded. For ledge and platform tests, the time the animal was able to balance on an acrylic ledge (0.75 cm wide and 30 cm high), and on a wooden platform (1.0 cm thick, 3.0 cm in diameter and elevated 47 cm) was recorded, respectively. The pole test was used to evaluate fine motor coordination by quantifying time to turn 180° and climb down a vertical pole. The screen tests assessed a combination of coordination and strength by quantifying time to climb up or hang onto a mesh wire grid measuring 16 squares per 10cm, elevated 47cm and inclined (60° or 90°) or inverted.

2.12.3 | Morris water maze—MWM was conducted as previously described (Wozniak et al., 2004). Briefly, cued, place and probe trials were conducted in a galvanized steel pool, measuring 120 cm in diameter, and filled with opaque water (diluted nontoxic white tempera paint). The PVC escape platform measured 11.5 cm in diameter. A digital video camera connected to a PC computer and the computer software program ANY-maze (Stoelting Co.) tracked the swimming pathway of the mouse to the escape platform and quantified path length, latency to find escape platform, and swimming speeds.

On two consecutive days, animals received four cued trials, separated by 1 hr, during which a red tennis ball atop a rod was attached to the escape platform and served as a visual cue. To prevent spatial learning, the escape platform was moved to a different quadrant location for each trial. The mouse was released from the quadrant opposite to the platform location and allowed 60s to locate the platform. Once the mouse found the platform, it was allowed to remain there for 10s before being returned to its home cage. Three days following visible platform testing, the cue was removed from the platform and it was submerged 1 cm under the water for the hidden platform tests. Animals received two blocks of two consecutive trials on five consecutive days, with an inter-trial interval between 30–90s and approximately 2 hr separating trial blocks. The escape platform remained in the same quadrant location for all trials and distal cues were placed on the walls of the room to support spatial learning. The mouse was released from a different location for each trial on each day. The mouse was allowed 60s to find the escape platform and allowed to sit on it for 10s before being returned to its home cage. Cued and hidden platform trials were combined into blocks of two or four trials for analyses, respectively. Following completion of hidden platform trials on the 5th day of training, the escape platform was removed from the pool and one 60s probe trial was conducted to assess memory retention for the location of the platform.

2.13 | Elevated plus maze

EPM was conducted as previously described (Wozniak et al., 2013). Briefly, a 5-min trial was conducted on each of 3 consecutive days. Animals were placed on a dimly lit black acrylic surface measuring 5 × 5 cm and elevated 63 cm above the floor equipped with photo beam pairs. Four arms (35 cm long, 5 cm wide; two open and two with 15 cm high walls)

extended from a central area. The MotorMonitor software (Kinder Scientific, LLC) quantified beam breaks as duration, distance traveled, entries, and time at rest in each zone (closed arms, open arms and center area).

2.13.1 | Novel object recognition—Pilot studies were conducted to evaluate the level of interest of specific objects and two different objects showing equal interest levels were chosen for this study (glass votive and metal basket) similar to (Yuede et al., 2009). Mice were habituated to the test arena (8.5 × 17 × 8 in) for 20 min per day, 2 days before testing. Each mouse received a sample trial and a test trial and novel and familiar objects were counterbalanced across genotypes and treatment groups. During the sample trial mice were placed in a familiar arena with 2 copies of the same object and allowed to explore for 10 min then returned to their home cage. Following 50-min delay mice, were placed back in the arena where a novel object was presented with one of the familiar objects explored during the sample trial and allowed to explore for 10 min. Objects and test arena were cleaned with 2% chlorhexidine after each trial. ANYMaze software (Stoelting Co., Wood Dale, IL) was used to track the location of the animal's head within the arena, and a 2-cm zone around each object. Active investigation was defined as facing the object within close proximity (2 cm). The amount of time spent investigating the novel object as compared to the familiar object was analyzed as a measure of recognition memory as described previously (Dere et al., 2005). Novelty preference scores were derived by calculating the percentage of the total investigation time spent investigating the novel object for each animal during the first minute.

2.13.2 | Experimental design and statistical analysis—Data in figures are presented as mean ± *SEM*. All statistical analysis was performed using Prism version 8.1 for Windows (GraphPad). Sample sizes were determined based on a power calculation of similarly-designed previous studies. For microdialysis studies where ISF Aβ levels are normalized to steady-state levels of each mouse, we need $n = 8$ mice per group to detect a 10% change in Aβ levels ($\alpha = 0.05$; power = 80%) {Cirrito, 2020 #1617}. For chronic treatment studies comparing absolute levels of Aβ between groups, $n = 12$ mice (mixed sex) per group are needed to detect a 20% change in Aβ plaque load and brain Aβ levels {Cirrito, 2011 #1008}. Statistical analyses were conducted by an experimenter other than the experimenter collecting the data. For analysis of microdialysis data at endpoints, the final 3 data points for a given treatment phase were averaged to assess overall effect of the drug and statistically compared to vehicle-treated mice at the same time point. One-way ANOVA analyses were performed with Dunnett's corrections for multiple comparisons. Comparison of only two groups was performed using a two-tailed, unpaired Student *t*-test method. No test for outliers was used and no data points were removed from analysis.

For behavior tests, statistical analyses were performed using IBM SPSS Statistic software (v.24), and GraphPad Prism (v8). Prior to analyses, all data were screened for fit of distributions with assumptions underlying univariate analyses, which included the Shapiro-Wilk test and q-q plot investigations for normality. Means and standard errors were computed for each measure. Analysis of variance (ANOVA), including repeated measures, and independent samples *t*-tests were used to analyze behavioral data. With a statistically

significant interaction between main factors, simple main effects were calculated to provide clarification of statistically significant between-subjects and within-subjects differences. Where appropriate, the Huynh-Feldt adjustment was used to protect against violations of sphericity, the Bonferroni correction was applied to multiple pairwise comparisons. Statistical results were confirmed with two-tailed non-parametric testing, when available, for any datasets with violations of the univariate assumptions. Probability value for all analyses was $p < .05$, unless otherwise stated.

3 | RESULTS

3.1 | $5HT_{2A}$-R inverse agonists suppress ISF Aβ levels

We used in vivo microdialysis to measure the dynamics of brain ISF Aβ over time in living mice (Cirrito et al., 2003; Fisher et al., 2016). This method allows serial collection of ISF Aβ every hour for up to 3–5 days in freely moving animals. Young, pre-plaque APP/PS1 mice were implanted with microdialysis probes into the hippocampus followed by a recovery period then measurement of baseline ISF Aβ levels in each mouse. While this model does not recreate all aspects of AD, these transgenic mice are a good model of APP processing and amyloidosis. Mice were then treated with Pim at three consecutive doses (0.1, 0.3, 1 mg/kg s.c) every 24 hr (Figure 1a). There was a dose-dependent decrease in ISF Aβ with a maximal suppression of Aβ by 47.4 ± 4.6% at the highest dose ($p < .0001$). Pim (0.3 mg/kg) had a similar maximal suppression of both ISF $Aβ_{40}$ and (34.6 ± 3.4% and 39.4 ± 8.2%, respectively) (Figure 1b). Both Aβ species reached their lowest levels by hour 9 with the Aβ levels returning to baseline levels by hour 60 after a single drug administration.

Although Pim has 30 to 50-fold selectivity for $5HT_{2A}$-R over $5HT_{2C}$-R in functional assays (Hacksell et al., 2014; Vanover et al., 2006), it is possible that its actions at $5HT_{2C}$-Rs contribute to the Aβ lowering effects of Pim. To assess the specificity of this effect for the $5HT_{2A}$-R, we treated mice with M100907 (M100) which lacks appreciable activity at $5HT_{2C}$-Rs (Kehne et al., 1996; Vanover et al., 2006; Weiner et al., 2001). Mice were administered with four consecutive doses of M100 (0.1, 0.3, 1.0, 3.0 mg/kg i.p.) 12 hr apart (Figure 2a). M100 had a maximal effect on ISF Aβ at 1.0 mg/kg with a 40.7 ± 3.9% (mean ± *SEM*) decrease compared to vehicle-treated mice ($p < .0001$), very similar to the maximal effect of Pim on Aβ. Mice were also administered a selective $5HT_{2C}$-R antagonist (SB242084), and a selective $5HT_{2C}$-R inverse agonist (SB206553), and neither compound had any effect on ISF Aβ levels (Figure 2b). We also assessed the effect of Pim in wildtype mice expressing murine Aβ (Figure 2c). Pim (1.0 mg/kg s.c.) decreased murine Aβ by 45.6 ± 5.8% compared to vehicle-treated mice ($p = .0002$). Importantly however, Pim had no effect in mice lacking $5HT_{2A}$-R expression, demonstrating the specificity of this effect to $5HT_{2A}$-R signaling.

3.2 | $5HT_{2A}$-R inhibition requires NMDA-R and ERK to regulate ISF Aβ

Synaptic transmission can directly cause Aβ generation by increasing APP endocytosis into the presynaptic terminal with subsequent cleavage into Aβ (Cirrito et al., 2008). Because $5HT_{2A}$-Rs can regulate neuronal excitability, we postulated Pim reduced Aβ by suppressing synaptic activity. In APP/PS1 mice, we first infused tetrodotoxin (TTX), a sodium channel

blocker, directly into the hippocampus via reverse microdialysis for 6 hr, followed administration of Pim. TTX permits postsynaptic activation but blocks action potentials and subsequent evoked synaptic transmission. As we have reported previously (Cirrito et al., 2005), TTX alone dramatically reduces synaptic activity and suppresses ISF Aβ levels by 33.5 ± 6.7% (Figure 3a). Interestingly however, despite the presence of TTX, Pim still significantly reduced ISF Aβ levels by an additional 28% ($p = .008$), suggesting that Pim does not require synaptic transmission to alter Aβ.

Previously, we demonstrated a dose-dependent effect of activating NMDA-R on Aβ (Verges et al., 2011) . High doses of NMDA activate extracellular-regulated kinase (ERK) to increase α-secretase activity and suppress Aβ (Hoey et al., 2009; Verges et al., 2011). Inhibition of NMDA-Rs with the potent NMDA-R antagonist MK801 completely blocked the effect of Pim on ISF Aβ (Figure 3b). However, memantine, which primarily inhibits extrasynaptic NMDARs, did not block the effect of Pim; ISF Aβ levels were still reduced by 25% and were not significantly different from vehicle-treated mice, suggested that synaptic NMDARs are responsible for altering APP processing into Aβ. Inhibition of ERK with FR180204 pre-treatment also blocked the effect of Pim on ISF Aβ levels (Figure 3c). In contrast, inhibition of protein kinase A (PKA) with KT5720 alone significantly increased ISF Aβ similar to ERK inhibition ($p = .050$), but did not block the effects of Pim on ISF Aβ levels (Figure 3c). This suggests that PKA may regulate Aβ levels, but does not mediate the effects of $5HT_{2A}$-Rs. These data demonstrate that NMDA-Rs and ERK are downstream of $5HT_{2A}$ signaling and required for $5HT_{2A}$-R mediated regulation of Aβ.

3.3 | Blockade of $5HT_{2A}$-Rs increases α-secretase activity

To determine how $5HT_{2A}$-R signaling alters ISF Aβ levels, we treated young APP/PS1 mice with vehicle or Pim (1 mg/kg s.c.) then 12 hr later sacrificed the animals and microdissected the hippocampus for biochemical analyses. We used western blot to assess changes in APP C-terminal fragments (CTF) α or β, and soluble APP-α fragments, and FRET-based peptide cleavage assays to measure the enzymatic activities of α-secretase and β-secretase. Although there was no change in APP CTF α or β, nor in soluble APP-α fragments (Figure 4a), the enzymatic activity of α-secretase was increased by 14% compared to vehicle-treated mice ($p = .005$) while there was no change in β-secretase activity (Figure 4b). The discrepancy between the unchanging APP-CTF α and a suppression in Aβ generation, could be because of the half-lives of each protein; the elimination of Aβ from the brain is almost twice as fast as soluble APP (Dobrowolska et al., 2014). These data suggest that Pim alters APP processing and Aβ generation by increasing α-secretase-dependent cleavage of APP.

3.4 | $5HT_{2A}$ signaling does not alter ISF Aβ elimination rate

A change in Aβ generation does not preclude a change in Aβ elimination as well. To directly determine if Pim alters Aβ clearance rate, we measured baseline ISF Aβ levels in APP/PS1 mice followed by vehicle or Pim for 9 hr, then administration of LY411575, a potent γ-secretase inhibitor, to rapidly block Aβ production within minutes (Cirrito et al., 2003). We then measured ISF Aβ for an additional 6 hr to measure the rate of clearance of existing Aβ (Figure 4c). The decline in ISF Aβ, as measured with microdialysis, follows first-order kinetics in both groups of mice (Figure 4d). The slope of the decline was then used to

calculate the in vivo Aβ elimination half-life of Aβ (Cirrito et al., 2003). Despite Pim-treated mice having a lower starting Aβ concentration, the elimination half-life of ISF Aβ was nearly identical with 1.34 ± 0.09 hr and 1.36 ± 0.09 hr in vehicle and Pim treated mice, respectively, demonstrating that acute treatment with Pim lowers Aβ by reducing production, and not by increasing elimination rate (Figure 4e).

3.5 | Continual administration of Pimavanserin has a sustained effect on ISF Aβ

To determine if continuous administration of Pim would be as effective at lowering Aβ as bolus doses, we measured baseline ISF Aβ levels in young APP/PS1 mice using microdialysis, followed by slow infusion of vehicle or Pim at 3 mg kg day^{-1} or 6 mg kg day^{-1} subcutaneously using an Alzet osmotic pump (3.75 μg/hr and 7.5 μg/hr, respectively). Both doses of Pim significantly reduced Aβ levels by approximately 25% after 24 hr of administration, reaching a steady-state reduction of approximately 40% by 36 hr after the start of the infusion (Figure 5).

3.6 | Chronic Pim administration reduces Aβ levels and aggregation

APP/PS1 mice start to develop amyloid plaques at about 4.5 months, reaching substantial plaque development by 10 months of age. 6-month old APP/PS1 mice, an age where these mice have already started to develop amyloid plaque (Savonenko et al., 2003), were implanted with Alzet osmotic pumps to deliver vehicle (PBS, pH 6.5) or Pim at 3 mg kg day^{-1} subcutaneously (see Supp. Fig. S2 for timeline). Male and female littermate mice were randomized into three treatment groups. One group of mice was sacrificed at 6 months of age to determine starting brain Aβ levels (Start group). The other two groups were administered vehicle or Pim for 4 months and sacrificed at 10 months of age. Alzet model 2006 osmotic pumps deliver compound for 6 weeks, so were replaced every approximately 2.5–5 weeks. During the final 3 weeks of drug dosing, mice underwent a series of behavioral tests, then had CSF extracted via the cisterna magna and transcardially perfused with chilled PBS/heparin. One brain hemisphere was post-fixed in 4% paraformaldehyde then processed for histology while the other hemisphere was microdissected into hippocampus and cortex then frozen on dry ice for biochemical assays.

Plaque load (% area covered) was assessed histologically in the hippocampus and cortex. Vehicle-treated mice had a 3.4-fold and 3.8-fold increase in plaque load in hippocampus and cortex compared to littermates sacrificed 4 months prior (Figure 6a and b). Importantly, mice treated with Pim had a significant 34.4% and 33.6% reduction in plaque load compared to vehicle-treated mice ($p = .024$ and $p = .013$, respectively). Representative histology images demonstrate a generally even reduction of plaques throughout both brain regions (Figure 6c). The contralateral hippocampus was sequentially extracted in PBS, 1% Triton X-100, then 5M guanidine with $Aβ_{40}$ and $Aβ_{42}$ measured by sandwich ELISA. There was no difference in either Aβ species in the PBS and Triton X-100 fractions between treatment groups (Fig S1a and b), However, there was a significant reduction in Aβ levels in the guanidine-soluble fraction which is believed to represent the fraction contributing to the damaging pathology and plaque formation caused by Aβ (Figure 6d). Surprisingly, neither guanidine-soluble $Aβ_{40}$ or $Aβ_{42}$ differed between Start and Pim groups, suggesting that drug treatment returned Aβ to pretreatment levels. Analyzing both sexes together, there was a significant

reduction in guanidine-soluble $A\beta_{40}$ by 59.1 ± 5.3% and $A\beta_{42}$ by 74.1 ± 3.5% in Pim-treated mice compared to vehicle ($p = .0012$, $p = .0006$, respectively). Similarly, there were approximately 25% and 40% decrease in CSF $A\beta_{40}$ and $A\beta_{42}$ levels in Pim-treated mice (Figure 6e, $p < .0001$, $p = .0005$, respectively).

Because Aβ levels in males and females stratified substantially, we also analyzed both sexes separately. Pim had a greater effect at lowering Aβ levels and plaques in females than in males (Fig. S1c–h), however females had a much greater plaque load to begin with, consistent with what has been observed previously with this strain of mouse (Ordonez-Gutierrez et al., 2015). Though the magnitude of those changes varied between the sexes, the pattern of changes was identical, and all significant effects detected when the sexes were analyzed together were also significant for each gender analyzed separately (Fig. S1c–h) with the exception of plaque load in the cortex which was significantly reduced in females, but not in males (Fig. S1d).

3.7 | Chronic Pim treatment improves behavioral function in APP/PS1 mice

Behavior was assessed during the final 3 weeks of chronic Pim treatment. Mice were evaluated on measures of general activity, sensorimotor function, anxiety, learning, and memory. Overall, the APP/PS1 mice showed increases in anxiety-related behaviors and impairments in spatial learning and memory, and in declarative or recognition memory, while Pim treatment generally decreased anxiety related behaviors and restored cognitive function to levels observed in WT mice (Figure 7). No significant effects of genotype or Pim treatment were found on measures of sensorimotor function, balance and motor coordination, body weights, or motor strength tests.

Vehicle treated APP/PS1 mice show decreased exploration of the activity chamber compared to WT mice; this effect is reversed by Pim treatment (Main effect of Group $F(3, 56) = 3.576$, $p = .0194$) (Figure 7a). Pim treatment also increased exploratory behavior as indicated by time spent rearing (main effect of Group $F(3, 56) = 5.353$, $p = .0026$) (Figure 7b), and time in the center zone of the chamber [$F(3,56) = 6.146$, $p = 0.01$] (Figure 7c), indicating decreased anxiety-related behavior compared to vehicle treated APP/PS1 mice. Vehicle-treated APP/PS1 mice show significantly lower general exploratory activity in the open field test and less time rearing compared to both WT groups, while Pim treated APP/PS1 mice were not significantly different from WT. In addition, vehicle treated APP/PS1 mice also spent significantly less time in the center zone of the chamber suggestive of increased anxiety-related behavior compared to Pim treated APP/PS1 and WT littermates (Figure 7a–c). Overall these results demonstrate Pim treatment reduced anxiety-related behaviors in APP/PS1 mice.

Spatial learning and memory were assessed in a Morris Water Maze task. No differences were observed between groups in the visible platform version of this test indicating that all mice were able to perform this task similarly (Figure 7d), however, we found a significant main effect of Group ($p = .003$) and interaction between Group and Trial block ($p = .031$) in the distance traveled to find the hidden platform in the water maze trials. When the platform was submerged, vehicle-treated APP/PS1 mice were significantly impaired in this task (main effect of Group $F(3,56) = 5.229$, $p = .0030$; Interaction Group × Trial $F(12,224) = 1.94$, p

= .031), taking significantly longer path lengths than WT Pim (p = .0104) and WT VEH (p = .0229) with Pim-treated APP/PS1 mice not significantly different from either vehicle treated WT or vehicle treated APP/PS1 mice (Figure 7e). In a probe trial conducted at the end of the learning trials to evaluate spatial memory, Pim-treated APP/PS1 mice showed improved memory for the platform location compared to vehicle-treated APP mice as indicated by their significant bias for the target quadrant compared to the other quadrants (p = .0064; Figure 7f).

Recognition or declarative memory was tested in a novel object recognition test. Pim-treated APP/PS1 mice show significantly more investigation of the novel object compared to vehicle treated APP/PS1 mice (p = .0181, Figure 7h), suggesting improved recognition memory. Pim treated mice displayed a preference for the novel object over the familiar object while vehicle-treated APP/PS1 mice did not, however this comparison did not reach statistical significance (p = .089) (Figure 7g). Importantly, all groups showed similar levels of investigation time in this task (Figure 7i). Thus, chronic Pim treatment decreased anxiety-related behavior and improved memory function in APP/PS1 mice.

4 | DISCUSSION

Pimavanserin is a potent, selective $5HT_{2A}$-R inverse agonist and functional antagonist (Hacksell et al., 2014; Vanover et al., 2006) with lesser activity at $5HT_{2C}$-Rs, and no appreciable activity at over 70 other targets. In addition, Pim is FDA-approved for the treatment of hallucinations and delusions associated with Parkinson's disease (Cummings et al., 2018). M100907 has a similar pharmacological profile, and additionally has no appreciable activity at $5HT_{2C}$-Rs (Kehne et al., 1996; Vanover et al., 2006; Weiner et al., 2001). The Aβ-lowering effects of both drugs were completely abolished in $5HT_{2A}$-R knockout mice. Additionally, neither a selective $5HT_{2C}$-R antagonist (SB242084) nor a selective $5HT_{2C}$-R inverse agonist (SB206553) had any effect on Aβ levels. Together these data confirm a novel and specific role for $5HT_{2A}$-Rs in regulating Aβ.

Suppression of $5HT_{2A}$-R activity by Pim or M100907 reduced Aβ levels by up to 50% through a signaling pathway involving NMDA-Rs, ERK, and α-secretase. Similar to Pim, direct activation of NMDA-Rs also causes a long-lasting effect on ISF Aβ that persists beyond the acute signaling at the receptor (Verges et al., 2011). Acute treatment with Pim causes an increase in α-secretase activity, with no apparent increase in Aβ elimination rate, strongly suggesting that acute Pim treatment reduces Aβ production. Chronic administration of Pim significantly reduced Aβ plaque load and CSF Aβ levels with concomitant reductions in anxiety-related behaviors and restoration of cognitive abilities. The behavioral improvements very likely resulted from the plaque lowering effects of Pim, without requiring an acute effect of the drug because the behavioral tests were conducted several days after drug administration through the Alzet pumps had stopped. Interestingly, there was a larger effect in females than males; however, that is likely driven by females having a greater Aβ burden. Serotonin signaling has a complex relationship with Aβ regulation. Activation of 5HT receptor subtypes 4,6, and 7 directly suppress Aβ generation in an ERK-dependent manner (Fisher et al., 2016). Similarly, we found that the Aβ lowering effects of Pim and M100907, which required 5-HT_{2A}-Rs, were also ERK-dependent, however via a

different endogenous signaling pathway that proceeds indirectly through NMDA-R signaling. The differential effects of MK801, which blocks all NMDARs, and memantine, which preferentially blocks extrasynaptic NMDARs (Xia et al., 2010), suggests that synaptic receptors drive much of the Aβ regulation here. This is consistent with primarily synaptic NMDARS activating ERK (Kaufman et al., 2012).

$5HT_{2A}$-Rs are known to regulate sleep architecture, and drugs that suppress $5HT_{2A}$-R activity have been consistently found to promote slow-wave sleep (SWS) (Ancoli-Israel et al., 2011; Patel et al., 2018; Popa et al., 2005; Vanover & Davis, 2010). A reciprocal relationship between SWS and Aβ accumulation has been demonstrated, with interruptions in SWS leading to Aβ accumulation, and augmentation of SWS lowering Aβ accumulation (Ju et al., 2017, 2019). Pim increases slow wave sleep (Ancoli-Israel et al., 2011) and ameliorates sleep abnormalities associated with Parkinson's disease (Patel et al., 2018). Disrupted sleep is a common problem in AD as well, which likely contributes to disease risk (Vanderheyden et al., 2018). Similar to many AD patients, APP transgenic mice also have disrupted sleep when Aβ plaques are present (Roh et al., 2012). Brain Aβ levels fluctuate with the circadian rhythm; ISF and CSF Aβ levels are high during wakefulness and low during sleep (Huang et al., 2012; Kang et al., 2009; Lucey et al., 2017). Sleep deprivation rapidly increases Aβ levels in mice and in humans (Kang et al., 2009; Lucey et al., 2018), leading to earlier and greater plaque accumulation (Kang et al., 2009). Conversely, promotion of slow wave sleep in APP transgenic (Tg2576) mice reduces the accumulation of amyloid plaque (Kang et al., 2009). While the acute effect of Pim on Aβ is likely because of a reduction in Aβ production through its net effect of increasing α-secretase activity through the $5HT_{2A}$-R / NMDA-R / ERK signaling pathway described above, an additional effect of Pim on also increasing Aβ removal cannot be ruled out. Indeed, the chronic effect of Pim on lowering Aβ pathology could also potentially involve more efficient glymphatic flushing of the ISF leading to increased removal of Aβ, as would be expected to occur with improved sleep rhythms.

It is likely that a therapeutic agent targeting Aβ will need to be administered very early in the disease course to make an appreciable difference; hence, a drug with few side effects will be necessary. Pimavanserin is approved by the FDA to treat psychosis in Parkinson's disease (Cummings et al., 2018), has also demonstrated efficacy against psychosis in Alzheimer's disease (Ballard et al., 2019), and in a variety of other dementia subtypes (Foff et al., 2019), and has a favorable tolerability profile compatible with long-term administration. Like other selective $5HT_{2A}$-R inverse agonists, Pimavanserin restores sleep architecture and promotes slow wave sleep, effects that chronically may also reduce Aβ-related pathology. Numerous therapeutic strategies targeting Aβ, such as secretase inhibitors and Aβ immunotherapies, have largely failed in clinical trials because of toxicity or lack of efficacy. In contrast to those strategies, suppressing $5HT_{2A}$-R activity with selective drugs would be a means to modulate an endogenous pathway that naturally regulates Aβ, and may offer therapeutic benefits against the underlying pathology, as well as the neuropsychiatric symptoms of Alzheimer's disease.

Supplementary Material

Refer to Web version on PubMed Central for supplementary material.

ACKNOWLEDGEMENTS

Financial support came from ACADIA Pharmaceuticals Inc., NIH/NIA P50 AG00568 (JRC), NIH/NINDS P01 NS074969 (JRC), NIH/NIA R01 AG064902 (JRC), and the Rotary Club International COINS for Alzheimer's disease Research Trust (JRC). Experiments were conducted in compliance with the ARRIVE guidelines.

Abbreviations:

AD	Alzheimer's disease
ANOVA	analysis of variance
Aβ	amyloid-beta
CTF	C-terminal fragments
ERK	extracellular-regulated kinase
i.p.	intraperitoneal
ISF	interstitial fluid
KO	knockout
PBS	phosphate-buffer saline
Pim	Pimavanserin
PKA	protein kinase A
RRIDs	Research Resource Identifiers
s.c.	subcutaneous
SWS	slow-wave sleep
TTX	tetrodotoxin
WT	wildtype

REFERENCES

Ancoli-Israel S, Vanover KE, Weiner DM, Davis RE, & van Kammen DP (2011). Pimavanserin tartrate, a 5-HT(2A) receptor inverse agonist, increases slow wave sleep as measured by polysomnography in healthy adult volunteers. Sleep Medicine, 12, 134–141. 10.1016/j.sleep.2010.10.004 [PubMed: 21256805]

Ballard C, Youakim JM, Coate B, & Stankovic S (2019). Pimavanserin in Alzheimer's disease psychosis: Efficacy in patients with more pronounced psychotic symptoms. The Journal of Prevention of Alzheimer's Disease, 6, 27–33.

Beliveau V, Ganz M, Feng L, Ozenne B, Hojgaard L, Fisher PM, Svarer C, Greve DN, & Knudsen GM (2017). A high-resolution in vivo atlas of the human Brain's serotonin system. Journal of Neuroscience, 37, 120–128. [PubMed: 28053035]

Bero AW, Yan P, Roh JH, Cirrito JR, Stewart FR, Raichle ME, Lee JM, & Holtzman DM (2011). Neuronal activity regulates the regional vulnerability to amyloid-beta deposition. Nature Neuroscience, 14, 750–756. [PubMed: 21532579]

Cai Z, & Ratka A (2012). Opioid system and Alzheimer's disease. Neuromolecular Medicine, 14, 91–111. 10.1007/s12017-012-8180-3 [PubMed: 22527793]

Cirrito JR, Disabato BM, Restivo JL, Verges DK, Goebel WD, Sathyan A, Hayreh D, D'Angelo G, Benzinger T, Yoon H, Kim J, Morris JC, Mintun MA, & Sheline YI (2011). Serotonin signaling is associated with lower amyloid-{beta} levels and plaques in transgenic mice and humans. Proceedings of the National Academy of Sciences of the United States of America, 108, 14968–14973. [PubMed: 21873225]

Cirrito JR, Kang JE, Lee J, Stewart FR, Verges DK, Silverio LM, Bu G, Mennerick S, & Holtzman DM (2008). Endocytosis is required for synaptic activity-dependent release of amyloid-beta in vivo. Neuron, 58, 42–51. [PubMed: 18400162]

Cirrito JR, May PC, O'Dell MA, Taylor JW, Parsadanian M, Cramer JW, Audia JE, Nissen JS, Bales KR, Paul SM, DeMattos RB, & Holtzman DM (2003). In vivo assessment of brain interstitial fluid with microdialysis reveals plaque-associated changes in amyloid-beta metabolism and half-life. Journal of Neuroscience, 23, 8844–8853. [PubMed: 14523085]

Cirrito JR, Yamada KA, Finn MB, Sloviter RS, Bales KR, May PC, Schoepp DD, Paul SM, Mennerick S, & Holtzman DM (2005). Synaptic activity regulates interstitial fluid amyloid-beta levels in vivo. Neuron, 48, 913–922. [PubMed: 16364896]

Cummings J, Ballard C, Tariot P, Owen R, Foff E, Youakim J, Norton J, & Stankovic S (2018). Pimavanserin: Potential treatment For dementia-related psychosis. The Journal of Prevention of Alzheimer's Disease, 5, 253–258.

DeMattos RB, Bales KR, Parsadanian M, O'Dell MA, Foss EM, Paul SM, & Holtzman DM (2002). Plaque-associated disruption of CSF and plasma amyloid-beta (Abeta) equilibrium in a mouse model of Alzheimer's disease. Journal of Neurochemistry, 81, 229–236. [PubMed: 12064470]

Dere E, Huston JP, & De Souza Silva MA (2005). Episodic-like memory in mice: Simultaneous assessment of object, place and temporal order memory. Brain Research Brain Research Protocols, 16, 10–19. 10.1016/j.brainresprot.2005.08.001 [PubMed: 16185914]

Dobrowolska JA, Michener MS, Wu G, Patterson BW, Chott R, Ovod V, Pyatkivskyy Y, Wildsmith KR, Kasten T, Mathers P, Dancho M, Lennox C, Smith BE, Gilberto D, McLoughlin D, Holder DJ, Stamford AW, Yarasheski KE, Kennedy ME, … Bateman RJ (2014). CNS amyloid-beta, soluble APP-alpha and -beta kinetics during BACE inhibition. Journal of Neuroscience, 34, 8336–8346. [PubMed: 24920637]

Eriksen JL, Sagi SA, Smith TE, Weggen S, Das P, McLendon DC, Ozols VV, Jessing KW, Zavitz KH, Koo EH, & Golde TE (2003). NSAIDs and enantiomers of flurbiprofen target gamma-secretase and lower Abeta 42 in vivo. Journal of Clinical Investigation, 112, 440–449.

Farber NB, Hanslick J, Kirby C, McWilliams L, & Olney JW (1998). Serotonergic agents that activate 5HT2A receptors prevent NMDA antagonist neurotoxicity. Neuropsychopharmacology, 18, 57–62. 10.1016/S0893-133X(97)00127-9 [PubMed: 9408919]

Fisher JR, Wallace CE, Tripoli DL, Sheline YI, & Cirrito JR (2016). Redundant Gs-coupled serotonin receptors regulate amyloid-beta metabolism in vivo. Molecular Neurodegeneration, 11, 45. [PubMed: 27315796]

Foff E, Cummings J, Soto-Martin M, McEvoy B, & Stankovic S (2019). HARMONY relapse-prevention study: Pimavanserin significantly prolongs time to relapse of dementia-related psychosis. The Journal of Prevention of Alzheimer's Disease, 6, S30–S31.

Grimwood S, Hogg J, Jay MT, Lad AM, Lee V, Murray F, Peachey J, Townend T, Vithlani M, Beher D, Shearman MS, & Hutson PH (2005). Determination of guinea-pig cortical gamma-secretase activity ex vivo following the systemic administration of a gamma-secretase inhibitor. Neuropharmacology, 48, 1002–1011. [PubMed: 15857627]

Hacksell U, Burstein ES, McFarland K, Mills RG, & Williams H (2014). On the discovery and development of pimavanserin: A novel drug candidate for Parkinson's psychosis. Neurochemical Research, 39, 2008–2017. 10.1007/s11064-014-1293-3 [PubMed: 24682754]

Halberstadt AL, van der Heijden I, Ruderman MA, Risbrough VB, Gingrich JA, Geyer MA, & Powell SB (2009). 5-HT(2A) and 5-HT(2C) receptors exert opposing effects on locomotor activity in mice. Neuropsychopharmacology, 34, 1958–1967. 10.1038/npp.2009.29 [PubMed: 19322172]

Hettinger JC, Lee H, Bu G, Holtzman DM, & Cirrito JR (2018). AMPA-ergic regulation of amyloid-beta levels in an Alzheimer's disease mouse model. Molecular Neurodegeneration, 13, 22. [PubMed: 29764453]

Hoey SE, Williams RJ, & Perkinton MS (2009). Synaptic NMDA receptor activation stimulates alpha-secretase amyloid precursor protein processing and inhibits amyloid-beta production. Journal of Neuroscience, 29, 4442–4460. [PubMed: 19357271]

Holtzman DM, Morris JC, & Goate AM (2011). Alzheimer's disease: The challenge of the second century. Science Translational Medicine, 3(77), 77sr1. [PubMed: 21471435]

Huang Y, Potter R, Sigurdson W, Santacruz A, Shih S, Ju YE, Kasten T, Morris JC, Mintun M, Duntley S, & Bateman RJ (2012). Effects of age and amyloid deposition on Abeta dynamics in the human central nervous system. Archives of Neurology, 69, 51–58. [PubMed: 21911660]

Jakab RL, & Goldman-Rakic PS (1998). 5-Hydroxytryptamine2A serotonin receptors in the primate cerebral cortex: Possible site of action of hallucinogenic and antipsychotic drugs in pyramidal cell apical dendrites. Proceedings of the National Academy of Sciences, 95, 735–740. 10.1073/pnas.95.2.735

Ju YS, Ooms SJ, Sutphen C, Macauley SL, Zangrilli MA, Jerome G, Fagan AM, Mignot E, Zempel JM, Claassen J, & Holtzman DM (2017). Slow wave sleep disruption increases cerebrospinal fluid amyloid-beta levels. Brain, 140, 2104–2111. [PubMed: 28899014]

Ju YS, Zangrilli MA, Finn MB, Fagan AM, & Holtzman DM (2019). Obstructive sleep apnea treatment, slow wave activity, and amyloid-beta. Annals of Neurology, 85, 291–295. [PubMed: 30597615]

Kang JE, Lim MM, Bateman RJ, Lee JJ, Smyth LP, Cirrito JR, Fujiki N, Nishino S, & Holtzman DM (2009). Amyloid-beta dynamics are regulated by orexin and the sleep-wake cycle. Science, 326, 1005–1007. [PubMed: 19779148]

Kaufman AM, Milnerwood AJ, Sepers MD, Coquinco A, She K, Wang L, Lee H, Craig AM, Cynader M, & Raymond LA (2012). Opposing roles of synaptic and extrasynaptic NMDA receptor signaling in cocultured striatal and cortical neurons. Journal of Neuroscience, 32, 3992–4003. 10.1523/JNEUROSCI.4129-11.2012 [PubMed: 22442066]

Kehne JH, Baron BM, Carr AA, Chaney SF, Elands J, Feldman DJ, Frank RA, van Giersbergen PL, McCloskey TC, Johnson MP, McCarty DR, Poirot M, Senyah Y, Siegel BW, & Widmaier C (1996). Preclinical characterization of the potential of the putative atypical antipsychotic MDL 100,907 as a potent 5-HT2A antagonist with a favorable CNS safety profile. Journal of Pharmacology and Experimental Therapeutics, 277, 968–981.

Kim J, Onstead L, Randle S, Price R, Smithson L, Zwizinski C, Dickson DW, Golde T, & McGowan E (2007). Abeta40 inhibits amyloid deposition in vivo. The Journal of Neuroscience: The Official Journal of the Society for Neuroscience, 27, 627–633. [PubMed: 17234594]

Lesne S, Ali C, Gabriel C, Croci N, MacKenzie ET, Glabe CG, Plotkine M, Marchand-Verrecchia C, Vivien D, & Buisson A (2005). NMDA receptor activation inhibits alpha-secretase and promotes neuronal amyloid-beta production. Journal of Neuroscience, 25, 9367–9377. [PubMed: 16221845]

Lomakin A, Teplow DB, Kirschner DA, & Benedek GB (1997). Kinetic theory of fibrillogenesis of amyloid beta-protein. Proceedings of the National Academy of Sciences of the United States of America, 94, 7942–7947. [PubMed: 9223292]

Lucey BP, Fagan AM, Holtzman DM, Morris JC, & Bateman RJ (2017). Diurnal oscillation of CSF Abeta and other AD biomarkers. Molecular Neurodegeneration, 12, 36. [PubMed: 28478762]

Lucey BP, Hicks TJ, McLeland JS, Toedebusch CD, Boyd J, Elbert DL, Patterson BW, Baty J, Morris JC, Ovod V, Mawuenyega KG, & Bateman RJ (2018). Effect of sleep on overnight cerebrospinal fluid amyloid beta kinetics. Annals of Neurology, 83, 197–204. [PubMed: 29220873]

Miner LA, Backstrom JR, Sanders-Bush E, & Sesack SR (2003). Ultrastructural localization of serotonin2A receptors in the middle layers of the rat prelimbic prefrontal cortex. Neuroscience, 116, 107–117. 10.1016/S0306-4522(02)00580-8 [PubMed: 12535944]

Nitsch RM, Deng M, Growdon JH, & Wurtman RJ (1996). Serotonin 5-HT2a and 5-HT2c receptors stimulate amyloid precursor protein ectodomain secretion. The Journal of Biological Chemistry, 271, 4188–4194. 10.1074/jbc.271.8.4188 [PubMed: 8626761]

Ordonez-Gutierrez L, Anton M, & Wandosell F (2015). Peripheral amyloid levels present gender differences associated with aging in AbetaPP/PS1 mice. Journal of Alzheimer's Disease, 44, 1063–1068.

Patel N, LeWitt P, Neikrug AB, Kesslak P, Coate B, & Ancoli-Israel S (2018). Nighttime sleep and daytime sleepiness improved with pimavanserin during treatment of Parkinson's disease psychosis. Clinical Neuropharmacology, 41, 210–215. 10.1097/WNF.0000000000000307 [PubMed: 30303817]

Popa D, Lena C, Fabre V, Prenat C, Gingrich J, Escourrou P, Hamon M, & Adrien J (2005). Contribution of 5-HT2 receptor subtypes to sleep-wakefulness and respiratory control, and functional adaptations in knock-out mice lacking 5-HT2A receptors. Journal of Neuroscience, 25, 11231–11238. 10.1523/JNEUROSCI.1724-05.2005 [PubMed: 16339018]

Preller KH, Burt JB, Ji JL, Schleifer CH, Adkinson BD, Stampfli P, Seifritz E, Repovs G, Krystal JH, Murray JD, Vollenweider FX, & Anticevic A (2018). Changes in global and thalamic brain connectivity in LSD-induced altered states of consciousness are attributable to the 5-HT2A receptor. eLife, 7, 1–31.

Roh JH, Huang Y, Bero AW, Kasten T, Stewart FR, Bateman RJ, & Holtzman DM (2012). Disruption of the sleep-wake cycle and diurnal fluctuation of beta-amyloid in mice with Alzheimer's disease pathology. Science Translational Medicine 4:150ra122

Savonenko AV, Xu GM, Price DL, Borchelt DR, & Markowska AL (2003). Normal cognitive behavior in two distinct congenic lines of transgenic mice hyperexpressing mutant APP SWE. Neurobiology of Disease, 12, 194–211. 10.1016/S0969-9961(02)00012-8 [PubMed: 12742740]

Sheline YI, West T, Yarasheski K, Swarm R, Jasielec MS, Fisher JR, Ficker WD, Yan P, Xiong C, Frederiksen C, Grzelak MV, Chott R, Bateman RJ, Morris JC, Mintun MA, Lee JM, & Cirrito JR (2014). An antidepressant decreases CSF Abeta production in healthy individuals and in transgenic AD mice. Science Translational Medicine, 6:236re234

Vanderheyden WM, Lim MM, Musiek ES, & Gerstner JR (2018). Alzheimer's Disease and sleep-wake disturbances: Amyloid, astrocytes, and animal models. Journal of Neuroscience, 38, 2901–2910. 10.1523/JNEUROSCI.1135-17.2017 [PubMed: 29563238]

Vanover KE, & Davis RE (2010). Role of 5-HT2A receptor antagonists in the treatment of insomnia. Nature and Science of Sleep, 2, 139–150.

Vanover KE, Weiner DM, Makhay M, Veinbergs I, Gardell LR, Lameh J, Del Tredici AL, Piu F, Schiffer HH, Ott TR, Burstein ES, Uldam AK, Thygesen MB, Schlienger N, Andersson CM, Son TY, Harvey SC, Powell SB, Geyer MA, … Davis RE (2006). Pharmacological and behavioral profile of N-(4-fluorophenylmethyl)-N-(1-methylpiperidin-4-yl)-N'-(4-(2-methylpropyloxy)phen ylmethyl) carbamide (2R,3R)-dihydroxybutanedioate (2:1) (ACP-103), a novel 5-hydroxytryptamine(2A) receptor inverse agonist. Journal of Pharmacology and Experimental Therapeutics, 317, 910–918.

Verges DK, Restivo JL, Goebel WD, Holtzman DM, & Cirrito JR (2011). Opposing synaptic regulation of amyloid-beta metabolism by NMDA receptors in vivo. Journal of Neuroscience, 31, 11328–11337. [PubMed: 21813692]

Weiner DM, Burstein ES, Nash N, Croston GE, Currier EA, Vanover KE, Harvey SC, Donohue E, Hansen HC, Andersson CM, Spalding TA, Gibson DF, Krebs-Thomson K, Powell SB, Geyer MA, Hacksell U, & Brann MR (2001). 5-hydroxytryptamine2A receptor inverse agonists as antipsychotics. Journal of Pharmacology and Experimental Therapeutics, 299, 268–276.

Willins DL, Deutch AY, & Roth BL (1997). Serotonin 5-HT2A receptors are expressed on pyramidal cells and interneurons in the rat cortex. Synapse (New York, N. Y.), 27, 79–82. 10.1002/(SICI)1098-2396(199709)27:1<79:AID-SYN8>3.0.CO;2-A

Wozniak DF, Diggs-Andrews KA, Conyers S, Yuede CM, Dearborn JT, Brown JA, Tokuda K, Izumi Y, Zorumski CF, & Gutmann DH (2013). Motivational disturbances and effects of L-dopa administration in neurofibromatosis-1 model mice. PLoS One, 8, e66024. 10.1371/journal.pone.0066024 [PubMed: 23762458]

Wozniak DF, Hartman RE, Boyle MP, Vogt SK, Brooks AR, Tenkova T, Young C, Olney JW, & Muglia LJ (2004). Apoptotic neurodegeneration induced by ethanol in neonatal mice is associated with profound learning/memory deficits in juveniles followed by progressive functional recovery in adults. Neurobiology of Diseases, 17, 403–414. 10.1016/j.nbd.2004.08.006

Xia P, Chen HS, Zhang D, & Lipton SA (2010). Memantine preferentially blocks extrasynaptic over synaptic NMDA receptor currents in hippocampal autapses. Journal of Neuroscience, 30, 11246–11250. 10.1523/JNEUROSCI.2488-10.2010 [PubMed: 20720132]

Yan P, Bero AW, Cirrito JR, Xiao Q, Hu X, Wang Y, Gonzales E, Holtzman DM, & Lee JM (2009). Characterizing the appearance and growth of amyloid plaques in APP/PS1 mice. Journal of Neuroscience, 29, 10706–10714. 10.1523/JNEUROSCI.2637-09.2009 [PubMed: 19710322]

Yuede CM, Zimmerman SD, Dong H, Kling MJ, Bero AW, Holtzman DM, Timson BF, & Csernansky JG (2009). Effects of voluntary and forced exercise on plaque deposition, hippocampal volume, and behavior in the Tg2576 mouse model of Alzheimer's disease. Neurobiology of Diseases, 35, 426–432. 10.1016/j.nbd.2009.06.002

Zhang C, & Marek GJ (2008). AMPA receptor involvement in 5-hydroxytryptamine2A receptor-mediated pre-frontal cortical excitatory synaptic currents and DOI-induced head shakes. Progress in neuro-psychopharmacology & Biological Psychiatry, 32, 62–71. 10.1016/j.pnpbp.2007.07.009 [PubMed: 17728034]

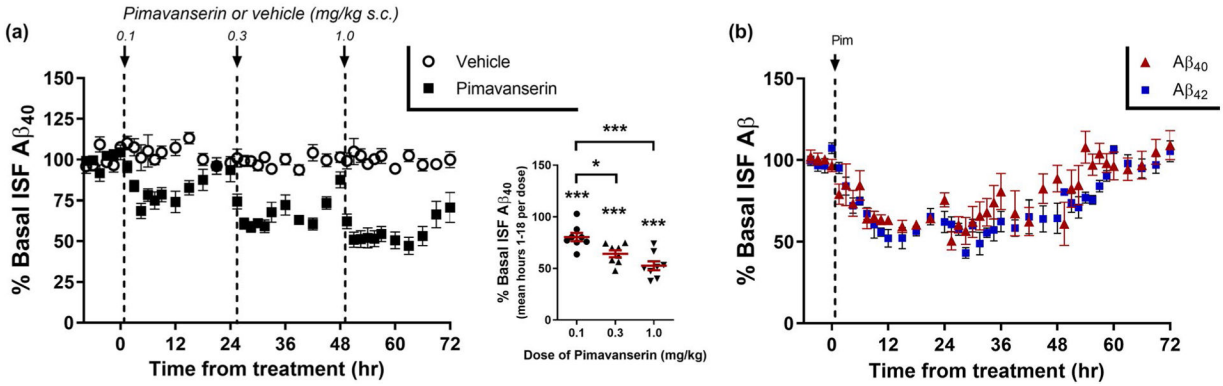

FIGURE 1.

$5HT_{2A}$ receptor inverse agonists suppress ISF Aβ levels. (a) 3- to 4-month-old APP/PS1 mice were implanted with in vivo microdialysis probes to assess ISF Aβ hourly over an 80 hr period. After 8 hr of baseline Aβ measurements, mice were injected 24 hr apart with Pimavanserin (s.c.) at 0.1 mg/kg, 0.3 mg/kg, and then 1.0 mg/kg. ISF $Aβ_{40}$ levels had a dose-dependent decrease of 23.4 ± 4.0% ($p = .0003$), 34.9 ± 3.4% ($p < .0001$), and 47.1 ± 4.4% ($p < .0001$), respectively, compared to vehicle-treated (PBS) mice during the same time period ($n = 8$ mice per group). (B) A single dose of 0.3 mg/kg (s.c.) Pimavanserin caused a maximal decrease in ISF $Aβ_{40}$ and $Aβ_{42}$ of 39.9 ± 2.4% and 46.2 ± 4.7%, respectively, from baseline by 12 hr after administration and returned to baseline levels by 54 hr after administration ($n = 6$ mice per group). The decrease in $Aβ_{40}$ and $Aβ_{42}$ was not significantly different between the two species ($p = .170$). Data present as mean ± *SEM*

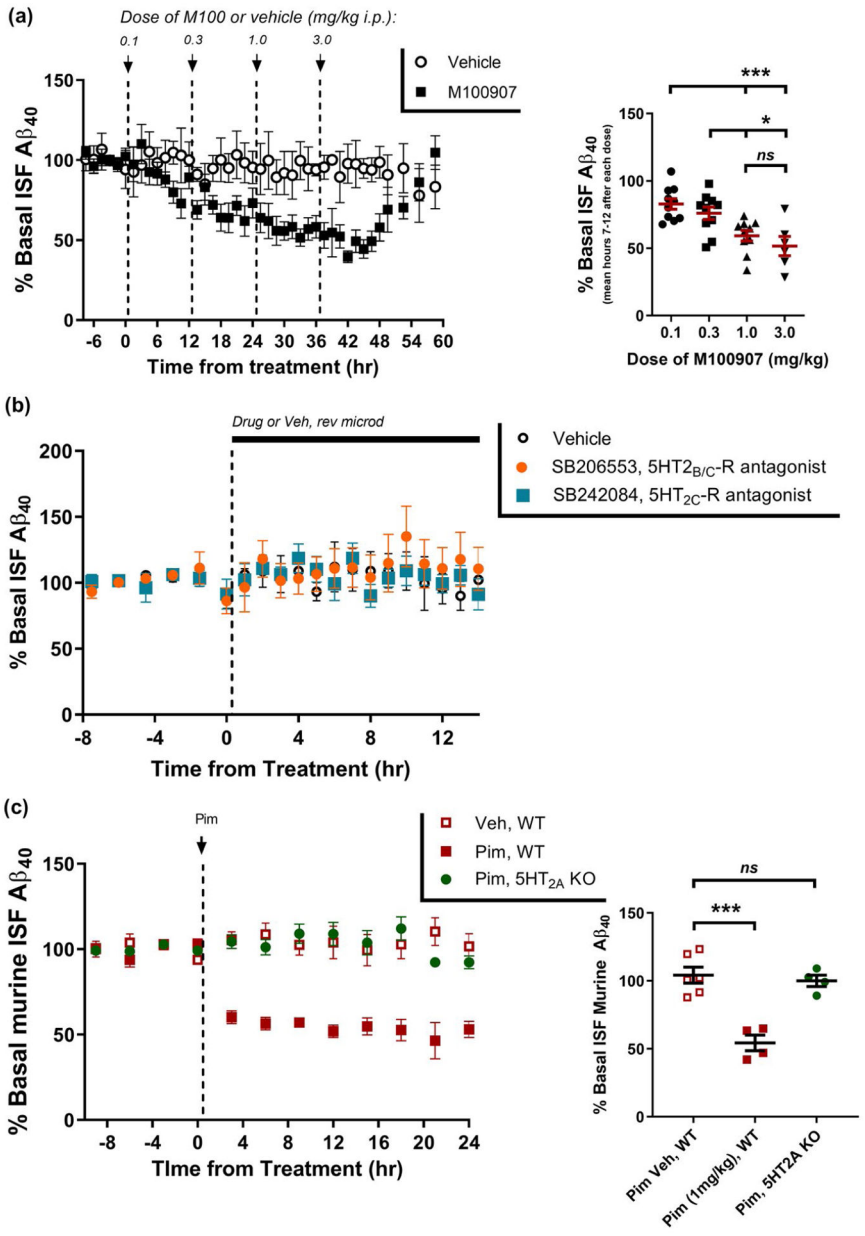

FIGURE 2.

Specificity of $5HT_{2A}$-R on Aβ regulation. (a) ISF $Aβ_{40}$ was measured by in vivo microdialysis following administration of M100907 (i.p.) every 12 hr at 0.1 mg/kg, 0.3 mg/kg, 1.0 mg/kg, and then 3.0 mg/kg. Aβ declined by 18.6 ± 3.9% (p = .063), 31.6 ± 4.7% (p = .0185), 46.2 ± 3.9% (p < .0001), and 56.6 ± 7.1% (p < .0001), respectively, at each of the doses compared to vehicle-treated mice at the during the same time period (n = 6–10 per group). (b) ISF $Aβ_{40}$ was assessed after administration of SB206553, a selective $5HT_{2B/C}$-R inverse agonist (1 μM) or SB242084, a selective $5HT_{2C}$-R antagonist (50 nM) by reverse microdialysis. Neither compound reduced ISF Aβ levels over a 14-hr period (n = 5–6 mice per group). (c) Murine Aβ in the ISF was measured in 3-month-old C57Bl/6 wildtype mice or $5HT_{2A}$-R knockout mice following administration of 1 mg/kg Pimavanserin (s.c.). Pim (1

mg/kg) reduced ISF $A\beta_{40}$ significantly in wildtype mice by 51.1 ± 5.8% (p = .0002), but had no effect in $5HT_{2A}$-R knockout mice (n = 4–6 mice per group). Data present as mean ± *SEM*

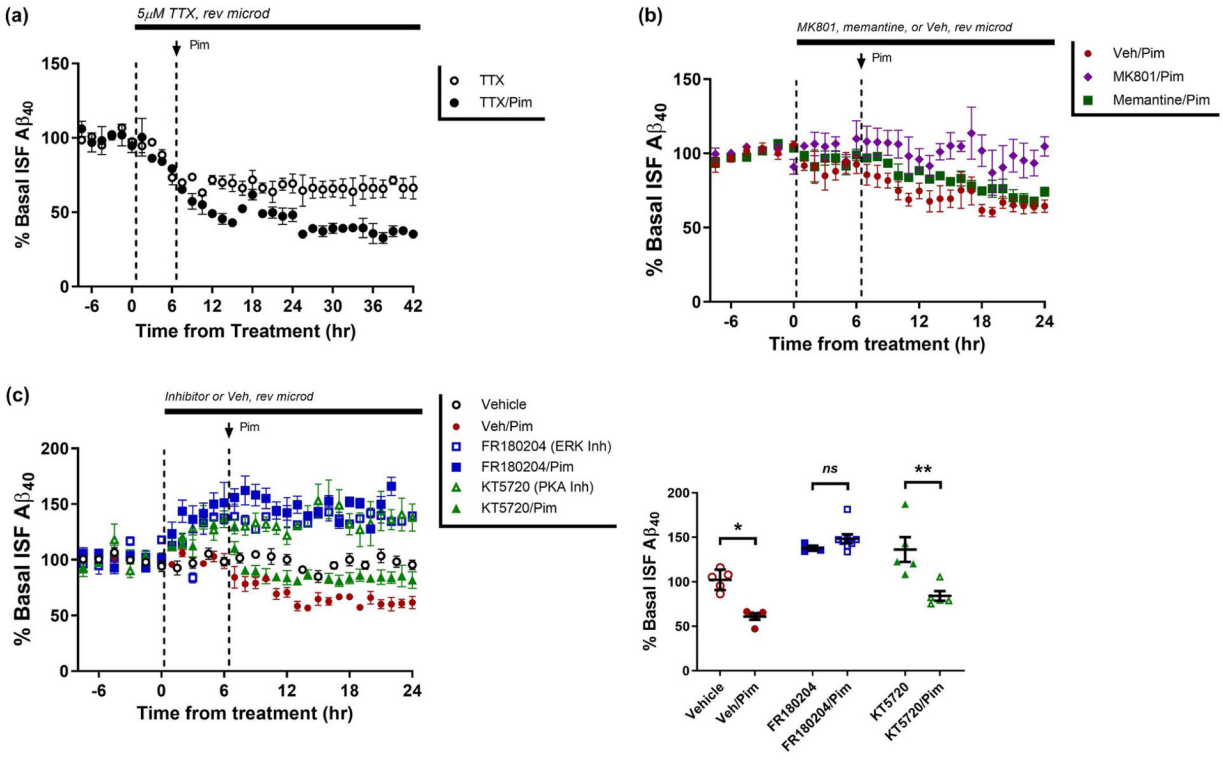

FIGURE 3.

Pimavanserin requires ERK activation to regulate ISF Aβ. (a) ISF Aβ was measured by microdialysis in young APP/PS1 mice at baseline, then pre-treated with tetrodotoxin (TTX) for 6 hr, followed by administration of vehicle or Pimavanserin (0.3 mg/kg s.c.). In TTX/vehicle-treated mice, ISF $A\beta_{40}$ was reduced by 33.5 ± 6.7% whereas in TTX/Pim mice it was reduced by 61.9 ± 2.7%. There as a significant difference in ISF Aβ in mice treated with vehicle versus Pim ($p = .008$; $n = 4$ per group). (b) After baseline measurement of ISF Aβ, mice were pre-treated with vehicle, MK801 (100 μM), or memantine (5 mg/kg ip), followed by Pimavanserin (0.3 mg/kg s.c.). In mice pre-treated with vehicle, Pim reduced ISF Aβ by 39.0 ± 3.5% ($p = .011$), however pre-treatment with MK801 completely blocked a Pim-induced change in Aβ ($n = 6$ mice per group). In mice pre-treated with memantine, by 24 hr ISF Aβ levels were still significantly reduced by 25.8 ± 3.1 compared to vehicle ($n = 7$; $p = .0035$), but were not statistically different from vehicle-treated mice ($p = .9419$). (c) Pretreatment with an ERK inhibitor (FR180204, 50 μM rev. microdialysis) alone increased ISF Aβ levels by 37.8 ± 2.9% ($p = .003$) over 30 hr, but a 6 hr pretreatment completely blocked the normal reduction of Aβ by Pim (10.7% difference between FR180204 alone and FR180204 with Pim; $p = .248$). In contrast, treatment with a PKA inhibitor (KT5720, 6 μM) increased ISF Aβ by 36.3 ± 13.9% ($p = .05$), but Aβ was still significantly reduced by 52.1% ($p = .008$) when KT5720 and Pim were co-administered compared to KT5720 alone ($n = 5$–8 mice per group). Data present as mean ± *SEM*

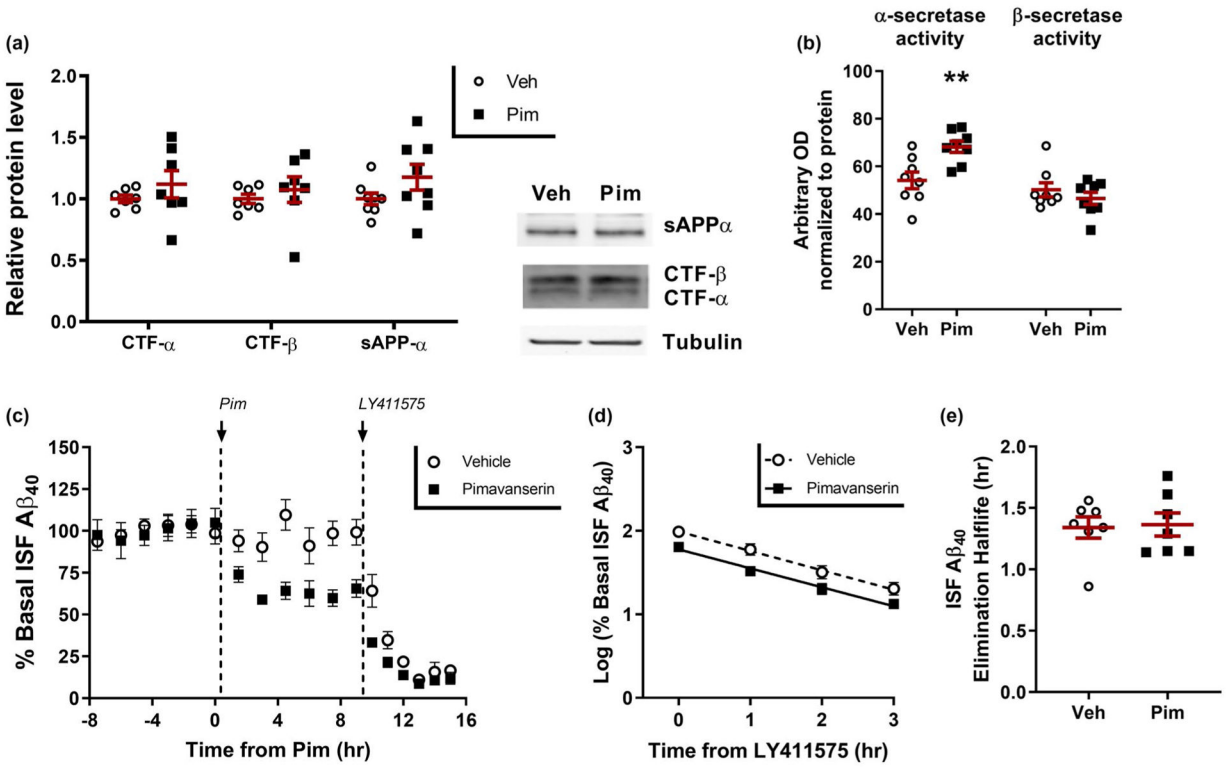

FIGURE 4.

Pimavanserin reduces Aβ production. Three months old APP/PS1 mice were administered vehicle (PBS) or Pimavanserin (1 mg/kg s.c.), sacrificed at 12 hr, with hippocampus microdissected and processed for biochemistry ($n = 8$ mice per group). (a) APP fragments were assessed by SDS-PAGE/Western blot. There was no significant difference in APP-CTF-β, APP-CTF-α, or soluble APP-α fragment in the Pimavanserin-treated mice. (b) Enzymatic activity of α-secretase was significantly increased by 26 ± 4.4% ($p = .005$) in Pimavanserin-treated mice, while there was no difference in β-secretase enzymatic activity. (c) In young APP/PS1 mice, ISF $A\beta_{40}$ was measured by microdialysis in mice pretreated with vehicle (PBS) or Pimavanserin (0.3 mg/kg s.c.) for 12 hr, followed by injection of a potent γ-secretase inhibitor (LY411575; 3 mg/kg i.p.) to rapidly block Aβ production (n 7 = 8 mice per group). (d) In both vehicle and Pim-treated mice, Aβ elimination followed first-order kinetics with (e) an Aβ elimination half-life of 1.34 ± 0.23 hr and 1.36 ± 0.09 hr, respectively, which did not differ significantly between the groups ($p = .861$). Data present as mean ± *SEM*

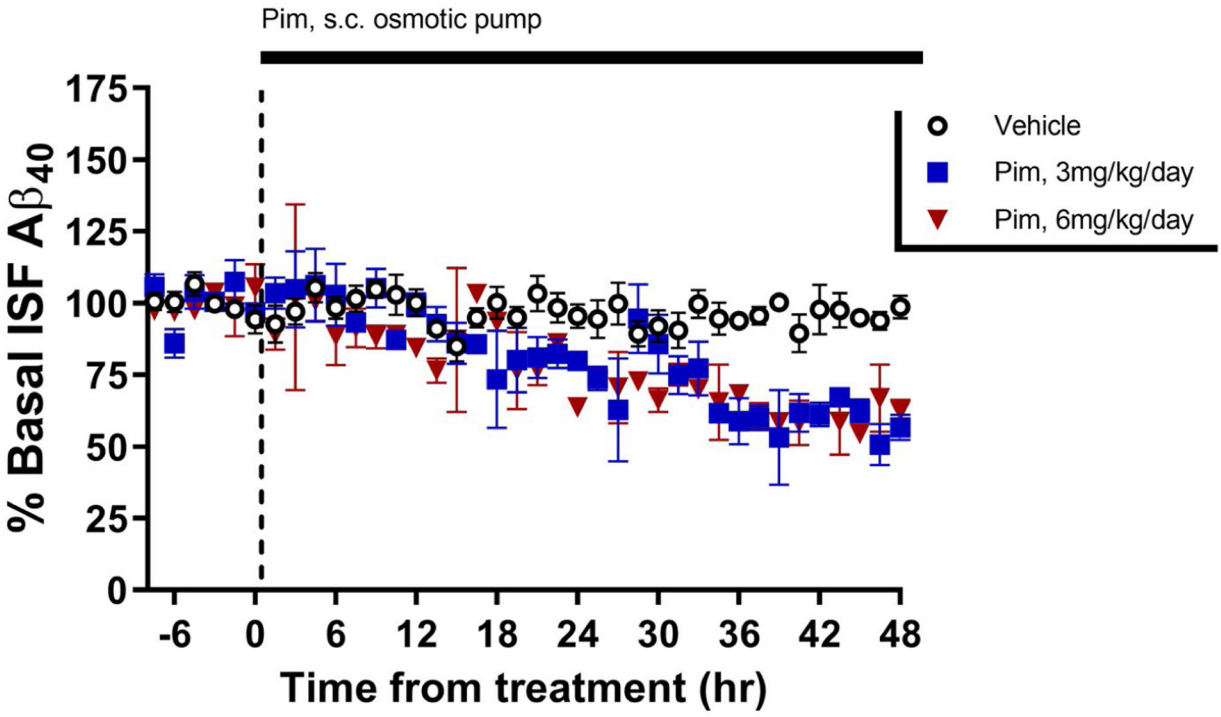

FIGURE 5.

Continual administration of Pimavanserin has a sustained effect on ISF Aβ. Young APP/PS1 mice has baseline ISF $A\beta_{40}$ measured by in vivo microdialysis for 8 hr followed by implantation of an Alzet osmotic pump subcutaneously on the back to continually administer vehicle or Pimavanserin at 3 mg kg day^{-1} or 6 mg kg day^{-1}. Aβ gradually declined to reach new, sustained levels of 40.4 ± 2.0% ($p = .001$) and 39.5 ± 4.9% ($p = .003$) in the treatment groups, respectively, by 36–48 hr after pump implantation compared to vehicle-treated mice ($n = 3–5$ mice per group). Data present as mean ± *SEM*

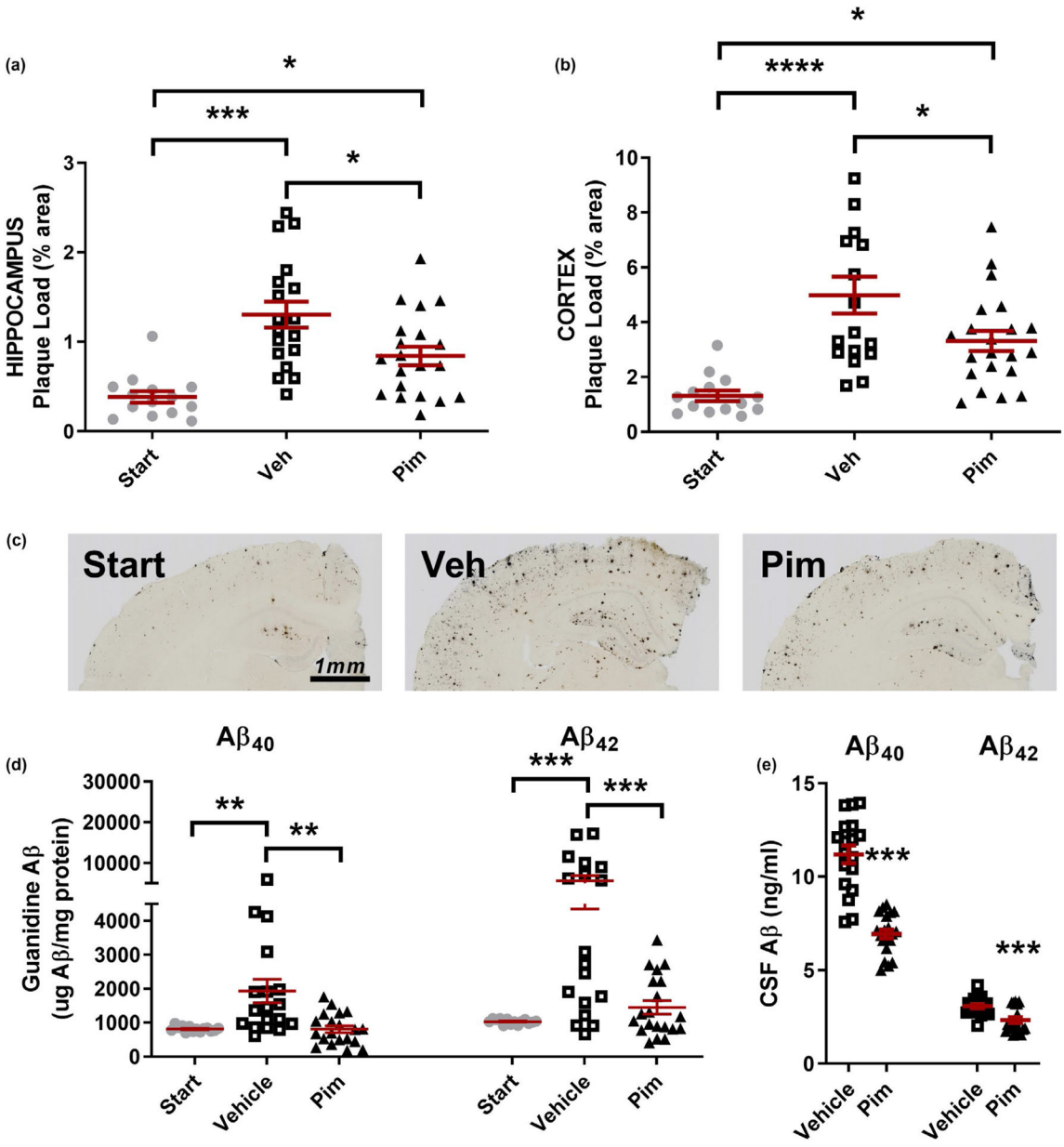

FIGURE 6.

Chronic Pimavanserin administration reduces Aβ levels and pathology. Six-month-old, plaque-bearing male and female littermate APP/PS1 mice were administered vehicle (PBS) or Pimavanserin (3.0 mg kg^{-1} day^{-1}) for 4 months by subcutaneous osmotic pump (n = 14–20 mice per group, mixed sex). One cohort of littermates was sacrificed at the beginning of drug treatment as a reference group (“Start” group). (a) Aβ plaque load (% area covered) in the hippocampus was assessed histologically. In the hippocampus, the Start, Vehicle, and Pimavanserin groups had 0.38 ± 0.06%, 1.3 ± 0.15%, and 0.84 ± 0.10% area covered, respectively, with all groups significantly different from each other. Pimavanserin reduced Aβ plaque load in the hippocampus by 35.5 ± 8.0% compared to vehicle-treated mice (p = .013). (b) In the cortex, the Start, Vehicle, and Pim groups had 1.3 ± 0.19%, 5.0 ± 0.67%,

and 3.3 ± 0.36% area covered, respectively. Pimavanserin reduced plaque load by 33.6 ± 7.3% compared to vehicle-treated mice ($p = .030$). (c) Representative histology images from each treatment group. (d) Guanidine-soluble Aβ in the hippocampus was significantly reduced in the Pimavanserin group compared to vehicle. In males, $A\beta_{40}$ and $A\beta_{42}$ were reduced by 44.9 ± 8.7% ($p = .0041$) and 40.3 ± 15.1% ($p = .0061$), respectively, and in females were reduced by 59.5 ± 4.5% ($p = .0355$) and 79.6 ± 3.1% ($p < .0001$), respectively. (e) CSF $A\beta_{40}$ and $A\beta_{42}$ was reduced by 39.1 ± 2.2% ($p < .0001$) and 24.2 ± 4.9% ($p = .0005$), respectively, compared to vehicle-treated mice. Data presented mean ± *SEM*

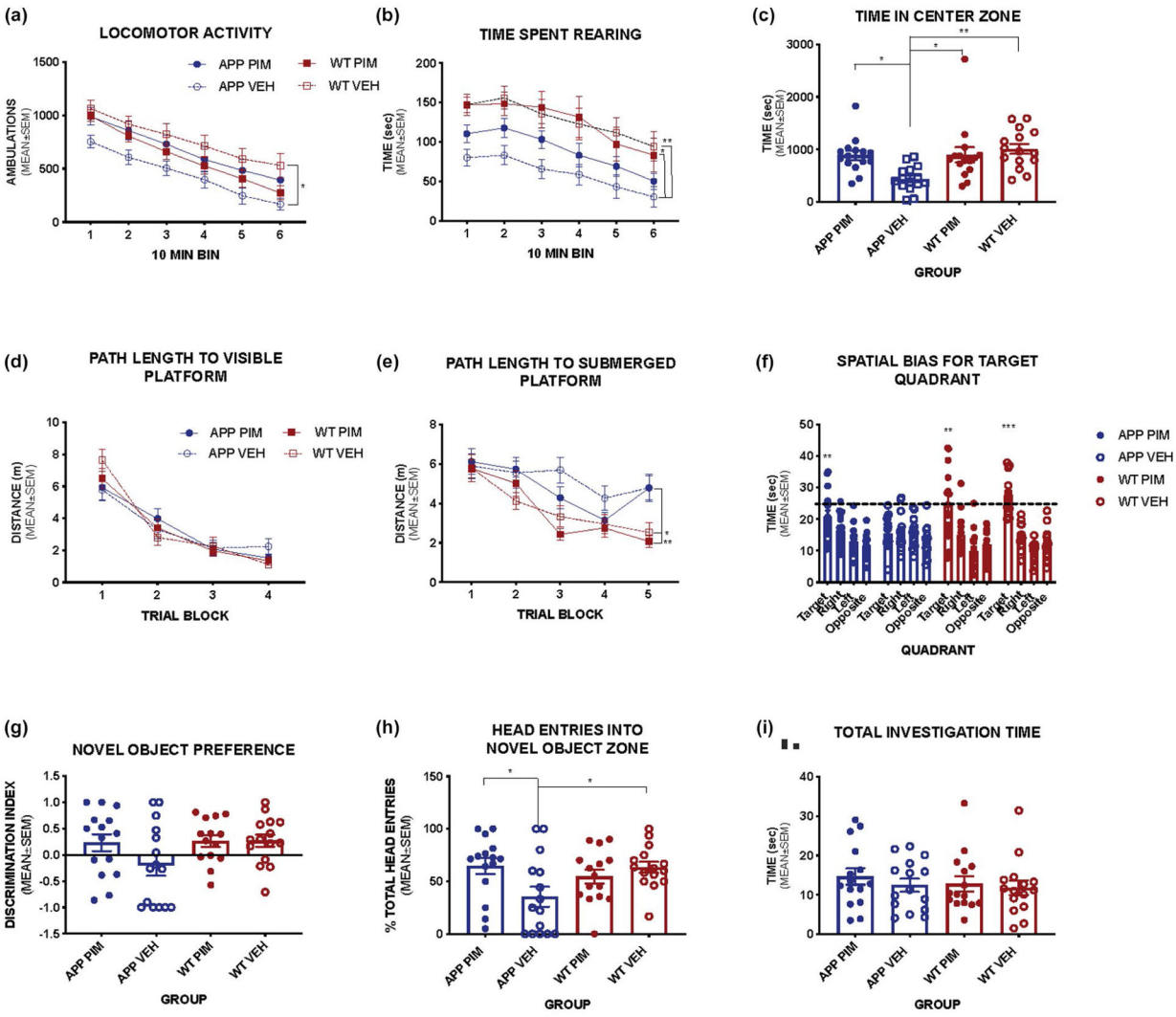

FIGURE 7.

Effect of chronic Pimavanserin on behavior. Chronic Pimavanserin treatment improves anxiety-related behavior and memory in APP/PS1 mice (n = 6–15 mice per group, mixed sex). (a) Vehicle treated APP/PS1 mice show decreased exploration of the activity chamber compared to WT mice, this effect is reversed by Pim treatment (Main effect of Group $F(3, 56) = 3.576$, $p = .0194$). (b) Pim treatment also increased exploratory behavior as indicated by time spent rearing (Main effect of Group $F(3, 56) = 5.353$, $p = .0026$), and in the center zone [$F(3, 56) = 6.146$, $p = 0.0.001$] of the chamber (c) indicating decreased anxiety-related behavior compared to vehicle treated APP/PS1 mice. (d) Path length to a visible escape platform is similar between groups [$F(3, 56) = 0.0293$, $p = .9932$], however when the platform is submerged, vehicle-treated APP/PS1 mice are significantly impaired on this task (E) (Main effect of Group $F(3,56) = 5.229$, $p = .0030$; Interaction Group × Trial $F(12, 224) = 1.94$, $p = .031$; APP/PS1 VEH mice took significantly longer path lengths than WT Pim $p = .0104$ and WT VEH $p = .0229$). (f) Pim treated APP/PS1 mice show intact spatial memory for the target location compared to all other quadrants in a probe trial [$F(2.004, 28.06) = 6.079$, $p = .0064$], while vehicle treated APP/PS1 mice do not [$F(2.363, 33.08) = 0.93$, p

= .4184]. (g) In the novel object recognition task, both WT groups and Pim treated APP/PS1 mice show preference for the novel object, while vehicle treated APP/PS1 mice do not. (h) Pim treated mice spend significantly more time investigating the novel object compared to vehicle-treated APP/PS1 mice [$F(3, 56) = 3.639$, $p = .0181$]. (i) Total investigation times are not different among groups [$F(3, 56) = 0.4207$, $p = .7388$]. (Bonferroni post hoc comparisons *$p < .05$, **$p < .01$, ***$p < .001$)